

Åkermanite based bioactive ceramics: structural and *in-vitro* bioactivity characterization

I. K. Mihailova*, L. N. Radev

University of Chemical Technology and Metallurgy, 8 St. Kliment Ohridski Blvd., 1756 Sofia

Received October 22, 2018; Accepted December 01, 2018

Ceramics with chemical composition corresponding to åkermanite ($2\text{CaO}\cdot\text{MgO}\cdot 2\text{SiO}_2$) was synthesized by using sol gel technique. The obtained dried gel was subjected to a two-step thermal treatment firstly at 700 °C for 2 hours and then at 1000, 1100, 1300 °C respectively for 2 hours. X-ray diffraction showed the temperature dependent structure evolution. The peculiarities of the crystallization of gels proceeding in the system $\text{CaO}\cdot\text{MgO}\cdot\text{SiO}_2$ provide the synthesis of materials of an identical chemical but with various phase composition, microstructure and relevant properties. All obtained samples from 700 to 1300 °C were multiphase. The quantity of åkermanite was increased with the increasing of the temperature.

The structural behavior of the synthesized after two-step thermal treatment at 700 and 1300 °C ceramics was examined by means of X-ray diffraction (XRD), Fourier Transform Infrared Spectroscopy (FTIR) and Scanning Electron Microscopy (SEM). Åkermanite, as the main crystalline phase, merwinite and diopside, as the minor phases, were identified. The XRD results were in good agreement with FTIR analysis.

The main purpose of the paper was the evaluation of the *in vitro* bioactivity of the åkermanite ceramics in static conditions for different periods of time – 7, 14 and 28 days in Simulated Body Fluid (SBF). The formation of carbonated apatite layer on the surface of the immersed samples was verified by FTIR, SEM and Energy Dispersive Spectroscopy (EDS) techniques. The change of ions concentrations in SBF was also carried out by Inductively Coupled Plasma Optical Emission Spectrometry (ICP-OES).

Keywords: $\text{CaO}\cdot\text{MgO}\cdot\text{SiO}_2$, ceramics, åkermanite, *in vitro* bioactivity.

INTRODUCTION

Over the last few decades, scientific research in the field of biomaterials has progressively increased. This is certainly due to scientific development and the opportunities offered by current research methods and equipment. On the other hand, the life expectancy of people in developed societies is increasing without necessarily eliminating their health problems. Regenerative medicine addresses precisely this problem by enabling for a higher quality of life for the elderly as well as for those who, due to trauma and illness, need medical treatment. This is all the more valid for bone regenerative medicine. The improvement and the development of new therapeutic approaches cannot be achieved without the development and application of new biomaterials. Biomaterials must comply with numerous and varying criteria, depending on the type of application.

Biomaterials function in direct contact with living tissues, in order to provide maximum support (stimuli) to the natural regenerative mechanisms of the body. To ensure this function, materials with appropriate chemical phase composition, structure and properties should be selected. For example, when developing implants for bone regeneration, one of the most important properties is their bioactivity, i.e. their ability to accumulate a mineral layer on the surface when placed in a biological environment, with a composition close to the mineral composition of the bone. This ensures that they can make a connection with the living bone.

Bioceramics in the $\text{CaO}\cdot\text{MgO}\cdot\text{SiO}_2$ system has been subject of a lot of research [1–14] that has identified them as promising for biomedical applications due to their *in vitro* and *in vivo* bioactivity, biodegradability, biocompatibility, etc. A number of studies have evaluated either the influence of the chemical composition (e.g. the magnesium content [1, 2]) or the phase composition by studying and comparing single-phase materials (e.g. bioceramics containing diopside [5, 6], åkermanite [7–9],

* To whom all correspondence should be sent:
E-mail: irena@uctm.edu

merwinite [10–11], bredigite [12–13], etc.). In this system, the strong impact was found of gels thermal treatment mode on crystallization and phase composition of the obtained glass-ceramic and ceramics [15]. This gives the opportunity to synthesize various materials containing crystalline phases in varying proportions without altering the chemical composition. Differences in the *in vitro* bioactivity of the synthesized materials could be expected given the effect of phase composition and structure on the properties of the materials. The purpose of this study is to synthesize and make a structural as well as *in vitro* bioactivity characterization of polyphase bioceramics with a chemical composition corresponding to Åkermanite. This study is a continuation of our previous research on polyphase materials produced by a similar method of synthesis but with a chemical composition corresponding to merwinite [16–17]. Applying the same approach in previous research and current study allows to make a comparison of the obtained *in vitro* bioactivity results.

EXPERIMENTAL

Sample preparation

Ceramics have been prepared with sol-gel method by using tetraethyl orthosilicate ((C₂H₅O)₄Si, TEOS), magnesium nitrate hexahydrate (Mg(NO₃)₂·6H₂O) and calcium nitrate tetrahydrate (Ca(NO₃)₂·4H₂O) as raw materials. Nitric acid (HNO₃, 2N) was used to catalyze the hydrolysis of TEOS. The TEOS was mixed with absolute ethanol, water and 2N HNO₃ (molar ratio: TEOS/H₂O/HNO₃=1:8:0.16) and hydrolyzed for 1 h under stirring. Then, the solutions of Ca(NO₃)₂·4H₂O and Mg₂(NO₃)₂·6H₂O were added into the mixture (molar ratio TEOS:Mg(NO₃)₂·6H₂O:Ca(NO₃)₂·4H₂O = 2:1:2), and reactants were stirred for 6 h at room temperature. After mixing, the solution was dried at 100 °C for 2 days to obtain the dry gel. The dried gel was calcined at 700 °C for 2 h. Finally, the powders were thermally treated at 1000, 1100, 1300 °C respectively for 2 h.

Characterization techniques

Thermal analysis was conducted to determine the temperature of heat treatment using a TG/ DTA system (STA PT1600 TG-DTA/DSC (STA Simultaneous Thermal Analysis) LINSEIS Messgerate GmbH Germany equipped with thermogravimetric (TG) and differential scanning calorimetry (DSC) units. The specimen was annealed at increasing temperature from 20 °C to 1000 °C in open air. The heating rate was set at 10°C/min.

X-ray powder diffraction (XRD) analysis was applied for phase identification. An X-ray diffractometer Philips at Cu K α radiation was used in the range from 8° to 90° 2 θ (step size: 0.05°, counting time per step: 1 s). The crystalline phases were identified using the powder diffraction files: PDF № 83-1815, PDF № 74-382 and PDF № 71-1067 from database JCPDS – International Centre for Diffraction Data PCPDFWIN v.2.2. (2001). The quantitative phase analysis was performed with the PowderCell 2.4 software [18].

FTIR spectroscopy has also been applied. Infrared transmittance spectra were recorded by using the pressed pellet technique in KBr. KBr pellets were prepared by mixing ~1 mg of the sample with 300 mg KBr. The measurements were made by a FTIR spectrometer Bruker Tensor 27 in the wave number/wavelength range from 4000 to 400 cm⁻¹. The transmittance spectra were recorded using MCT detector with 64 scans and 1 cm⁻¹ resolution.

The morphology of the surface and chemical composition were analyzed using Scanning Electron Microscopy SEM Hitachi SU-70 equipped with energy dispersive spectrometer (EDS).

In vitro test for bioactivity in SBF solution

In order to estimate the *in vitro* bioactivity (potential for apatite formation) of the sample, we used the Simulated Body Fluid (SBF) proposed by Kokubo et al. [19], the Tris-buffered SBF (Na⁺ 142.0, K⁺ 5.0, Mg²⁺ 1.5, Ca²⁺ 2.5, Cl⁻ 147.8, HCO₃⁻ 4.2, HPO₄²⁻ 1.0 and SO₄²⁻ 0.5 mol m⁻³; 7.4 pH). The concentration of various ions in the SBF was adjusted to be similar to those in human blood plasma.

0.3 g of the homogenized ceramic powders were uniaxially pressed to obtain pellets 2 mm in thickness and 10 mm in diameter. The pellets were placed in polyethylene bottles containing 20 ml of SBF at 37 ± 0.5 °C. The sample surface area to SBF volume (SA/V) ratio was equal to 0.1 cm⁻¹.

Pellets were removed after 7, 14 and 28 days of soaking, gently rinsed with deionized water and acetone, and dried at room temperature.

Sample surfaces and cross-sections, before and after SBF treatment, were examined by SEM and EDS. The changes in the samples during the *in vitro* test were also registered by FTIR spectroscopy.

The SBF was removed after several periods of immersion and calcium, magnesium, phosphorus, and silicon ion concentration in the removed SBF was determined by inductively coupled plasma optical emission spectrometry (Prodigy High Dispersion ICP-OES Spectrometer from Teledyne Leeman Labs – USA).

RESULTS AND DISCUSSION

Phase composition of the samples depending on the thermal treatment of the dry gel

The purpose of the first stage of thermal treatment was to decompose the nitrates and remove the residues of the solvents used after the gel-drying step. Its temperature was determined by DTA-TG analysis of the dry gel. The experimental DTA curve (Fig. 1) revealed endoeffects, accompanied by a mass loss up to 540 °C. Based on these data, the 700 °C temperature was determined for the first stage of the thermal treatment.

According to the results of the XRD analysis (Table 1), the crystallization of the gel with a composition of 2CaO.MgO.2SiO₂ (corresponding to the stoichiometry of Åkermanite) starts with the formation of Ca₂SiO₄ and Ca₃MgSi₂O₈ merwinite, i.e. crystalline phases that are richer in CaO compared to the composition of the starting gel. Such crystallization behavior of gel is characteristic for the CaO-MgO-SiO₂ system and according to [15] is due to the varying cation mobility. This determines system specificity and the significant effect of gel thermal treatment mode on the phase composition of the obtained glass-ceramics and ceramics. This system gives the opportunity to synthesize a wide

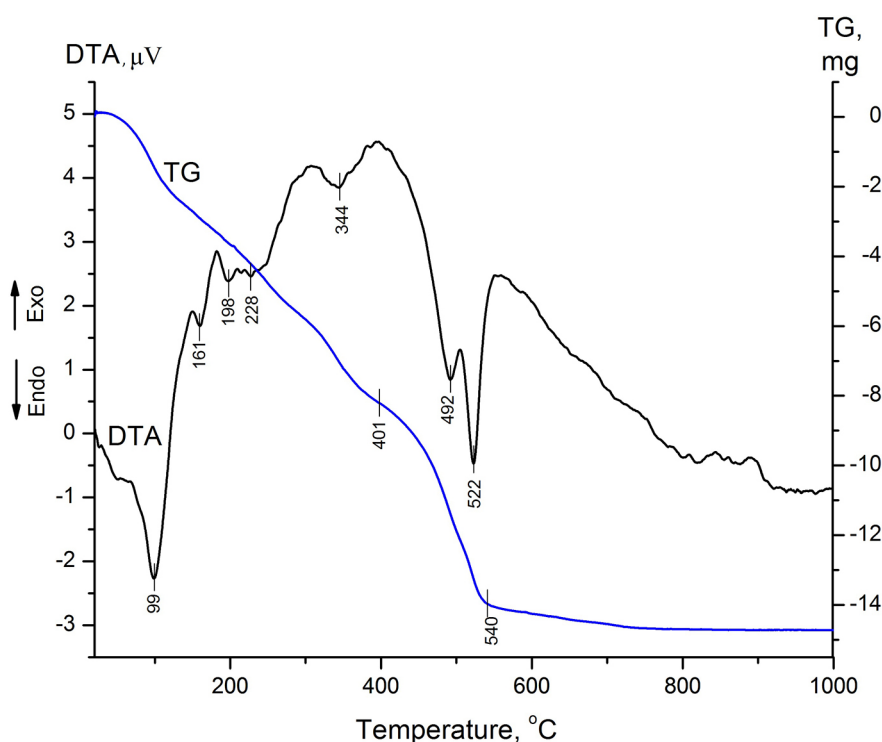


Fig. 1. Thermal (TG-DTA) analysis of the dry gel.

Table 1. Phase composition of the samples depending on the thermal treatment of the dry gel

Crystalline phases identified in the sample	Thermal treatment of dry gel			
	700°/2h	700°/2h + 1000°/2h	700°/2h + 1100°/2h	700°/2h + 1300°/2h
Åkermanite, Ca ₂ MgSi ₂ O ₇	–	16%	24%	57%
Diopside, CaMgSi ₂ O ₆	–	28%	26%	22%
Merwinite, Ca ₃ MgSi ₂ O ₈	30%*	54%	50%	21%
Larnite, β-Ca ₂ SiO ₄	56%*	–	–	–
Periclase, MgO	14%*	1.2%	–	–

* These are the ratios only between the crystalline phases, however there is a significant amount of amorphous phase in the sample that is not calculated.

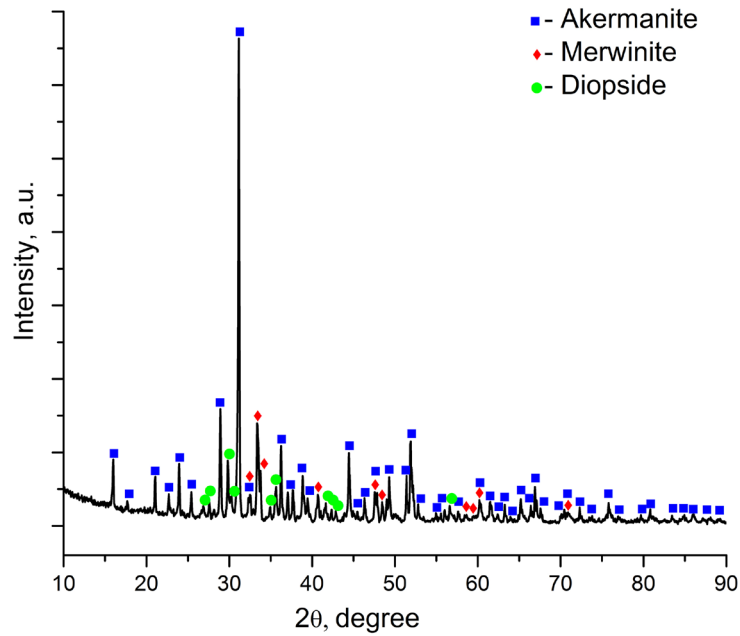


Fig. 2. X-ray diffraction pattern of the ceramics ÅBC.

variety of materials containing crystalline phases in varying proportions without altering the chemical composition. Given the effect of phase composition and structure on the materials bioactivity, differences in the *in vitro* bioactivity can be expected, both between the synthesized materials, as well as when compared to single-phase ceramics, which typically require continued thermal treatment at high synthesis temperatures.

Structure of åkermanite based ceramics (ÅBC)

In this study, ceramics obtained after thermal treatment at 1300 °C, hereinafter referred to as ÅBC (Åkermanite Based Ceramics), was selected in order to make a more detailed structural analysis and evaluation of the apatite forming ability in a SBF environment. As can be seen from Fig. 2 and Table 1, its phase composition is characterized by the predominant presence of åkermanite and the presence of similar amounts of merwinite and diopside. According to the literature data, the three phases exhibit suitable properties for biomedical applications [3–11].

The FTIR spectrum of ÅBC sample is presented in Fig. 3 (a). The vibrations of the $[\text{Si}_2\text{O}_7]^{6-}$ group in the åkermanite structure are positioned from 1020 to 600 cm^{-1} . The band at 1020 cm^{-1} is assigned to the antisymmetric stretching of oxygens in åkermanite, whereas the bands at 972, 933 and 905 cm^{-1} are assigned to symmetrical stretching modes of terminal oxygens [20]. The bands at 683 cm^{-1} and

587 cm^{-1} could be related to symmetrical stretching, $\nu_s(\text{Si-O-Si})$ mode of bridging oxygen of the pyrosilicate units, and to the presence of CaO group [20].

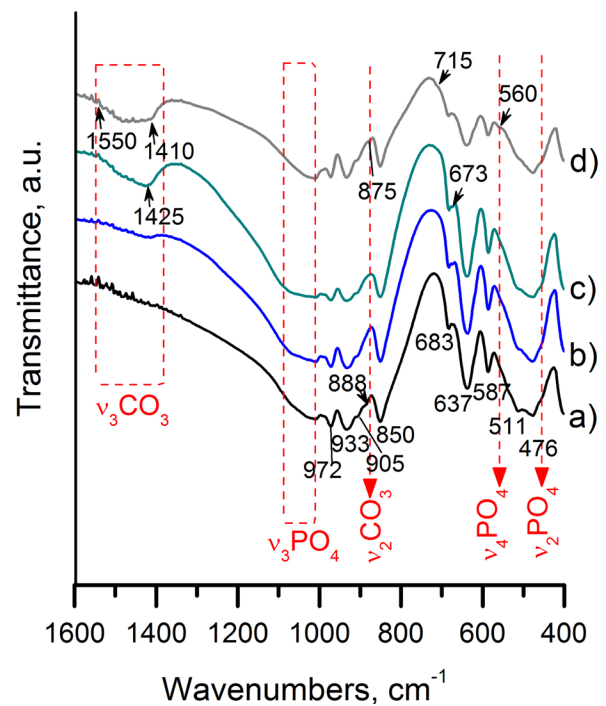


Fig. 3. FTIR spectra of the prepared ceramics ÅBC (a) and after its immersion in SBF for 7 (b), 14 (c) and 28 (d) days in static conditions.

The bands posited in the range 1050–850 cm^{-1} correspond to internal antisymmetric and symmetric stretching vibrations of SiO_4 tetrahedra in merwinite [21]. The peaks near 1020, 972, 933, 905 and 587 cm^{-1} in the FTIR spectrum of ÅBC correspond to the vibration modes of both phases [16, 20, 21].

The FTIR spectrum of pyroxene has a very characteristic pattern with three strong bands in the range of 1070 to 850 cm^{-1} . The adsorption at $\approx 1070 \text{ cm}^{-1}$ may be attributed to the $\nu_{\text{as}}(\text{Si-O-Si})$ mode in the diopside structure [22]. The bands at 972 and 850 cm^{-1} are due to the symmetrical

$\nu_{\text{s}}(\text{Si-O}^-)$ and antisymmetric $\nu_{\text{as}}(\text{Si-O}^-)$ stretching of the terminal nonbridging oxygens in the pyroxene chains. The band at 637 cm^{-1} corresponds to the symmetric stretching of bridging oxygen $\nu_{\text{s}}(\text{Si-O-Si})$ [22].

The other complex intensive bands in the region 550 to 450 cm^{-1} could be assigned to Si–O–Si bending vibration and to vibrations of the MgO_6 and MgO_4 groups [20]. The presented FTIR results are in good agreement with XRD analysis.

The microstructure of the ÅBC sample is shown in Fig. 4 (a) and (b). Micropores and polygonal

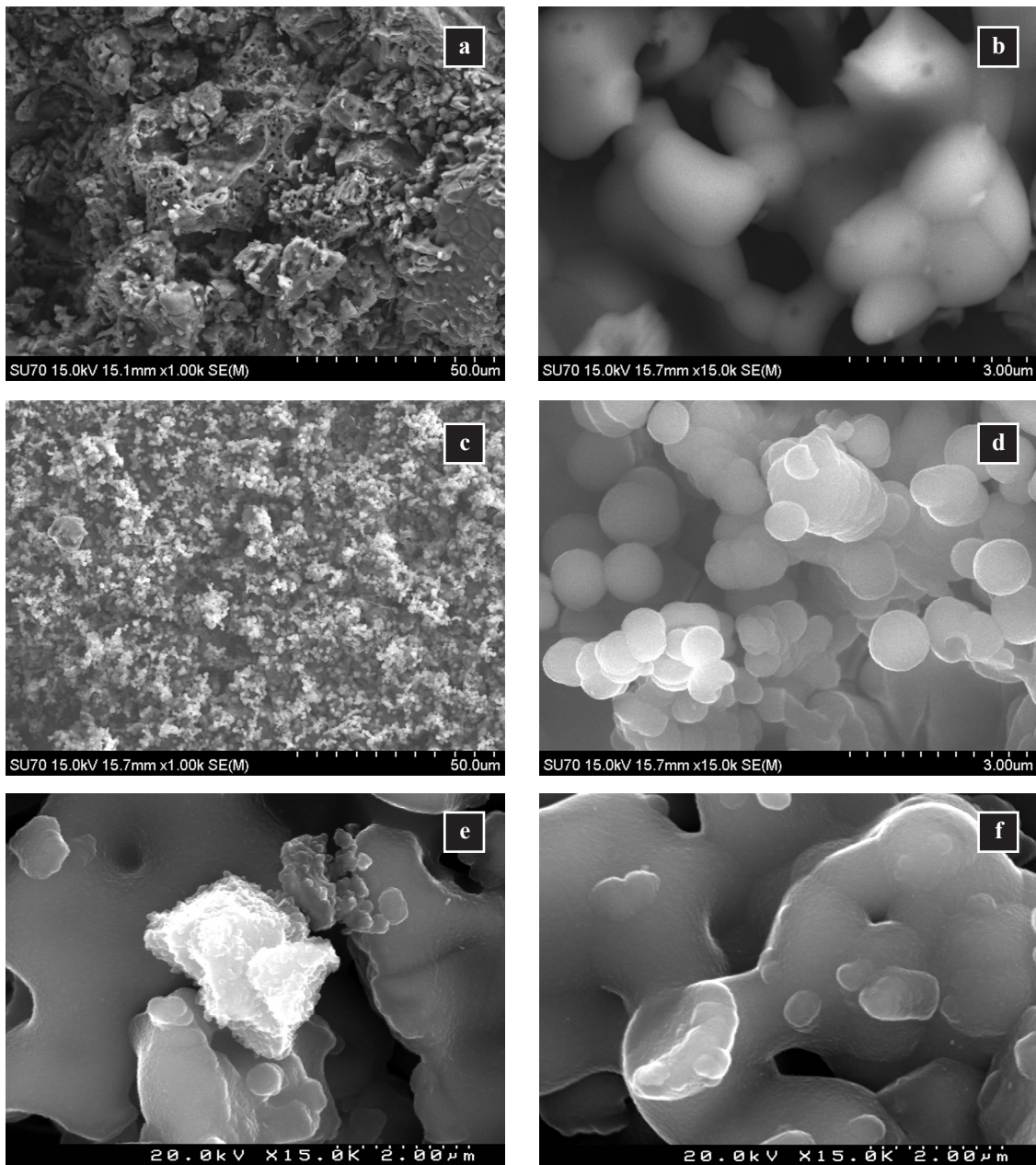


Fig. 4. SEM images of ÅBC-surface: as synthesized, i.e. before *in vitro* test (a)1000 \times , (b) 15000 \times ; and after soaking in SBF for 7 days (c) 1000 \times , (d) 15000 \times ; for 14 days (e) and for 28 days (f)

crystals with dimensions of 1–1.5 μm were found. The structural features are characteristic of liquid phase sintering.

In vitro bioactivity of Åkermanite based ceramics

The FTIR spectra of ÅBC after soaking in SBF up to 28 days (Fig. 3) show that the main spectral characteristics remain unchanged during the testing period. At the same time the results show a decrease in the relative intensity of some absorption bands, an increase in the intensity of others, and the appearance of new absorption bands in ceramics spectra with the increase in the time of soaking in SBF. These changes can be explained by the partial dissolution of the silicate phases and the formation of phosphates. Absorbance at 1100–1000 cm^{-1} relates to $\nu_3 \text{PO}_4^{3-}$, the new band at 560 cm^{-1} corresponds to $\nu_4 \text{PO}_4^{3-}$ and the shoulder at 460 cm^{-1} belongs to $\nu_2 \text{PO}_4^{3-}$. These vibrational modes are characteristic of the PO_4^{3-} ions in hydroxyapatite (HA) structure [23]. With the increase of the soaking time in SBF, the complex absorption band between 1500–1400 cm^{-1} rises, which is associated with the presence of carbonates [24]. Carbonate groups can substitute for $[\text{PO}_4]^{3-}$ and $(\text{OH})^-$ groups in the structure of hydroxyapatite, but they are also likely to form carbonate phases. After 28 days of soaking, absorption peaks at 875 and 715 cm^{-1} in the spectrum of the sample were also observed, which could also be attributed to a carbonate group [24].

SEM micrographs of the ÅBC surface after 7 days in SBF (Fig. 4. b, c) show a significant change. The surface is covered with newly formed spherical aggregates with the typical morphology of apatite. The sphere sizes reach up to 1 μm . The EDS data in Fig. 5 shows that the composition of the formed layer is calcium phosphate (Ca:P = 2,11)

According to the ICP results, no phosphorus content was detected in SBF after 7 days of soaking, i.e. the whole content was depleted within 7 days of soaking the ceramics, while the concentrations of Ca, Mg, Si have increased (Fig. 6) as a result of the dissolution of the ceramics phases.

The obtained results from FTIR, SEM, EDS and ICP-OES reveal the formation of an apatite layer on the ceramic surface after 7 days of soaking in SBF. Therefore, the studied ÅBC ceramics has *in vitro* bioactive properties.

According to some authors [20] the presence of merwinite in Åkermanite ceramics leads to a faster apatite layer formation compared to that in the single-phase Åkermanite. However, it is important to note that, besides the phase composition, material's bioactivity is affected by a number of other factors, e.g., the microstructural features of the material.

The absence of phosphorus in the solution after 7 days of soaking in SBF inhibits the further apatite deposition. On the other hand, the ICP data after 14 and 28 days of soaking in SBF show an increase in the concentration of Ca, thus indicating a continued process of dissolution and preferential passage of Ca from ceramics into the solution. The dissolution of ÅBC ceramics in SBF environment is a factor that enhances its bioactivity, making it promising for bone regeneration. During this time-frame, the deposition of the surface layer continues, with the possible inclusion of silicon and magnesium in the composition of the formed phases. This is in line with the ICP data that shows a reduction in the concentrations of these elements in the SBF. The corresponding ÅBC surface morphology after 14 and 28 days of soaking in SBF is illustrated in Fig. 4 (e, f)

Fig. 6 shows the evolution of SBF ion concentration during the *in vitro* soaking test of ÅBC, and for comparison purposes, our published results for merwinite ceramics MC1 [16] and MC2 [17]. MC1 merwinite ceramics (85% merwinite and 15% Åkermanite) is obtained by sol-gel synthesis similar to that used for ÅBC (including the same thermal treatment). Interesting results are obtained by comparing the *in vitro* bioactivity of both ceramics. SEM morphology analysis: the newly formed spherical aggregates after soaking in SBF for 7 days are very similar in type, size and distribution.

The Ca, Mg, Si ions concentration after soaking in SBF for 7 days is higher in the solution with Åkermanite ceramics (ÅBC) than that with merwinite

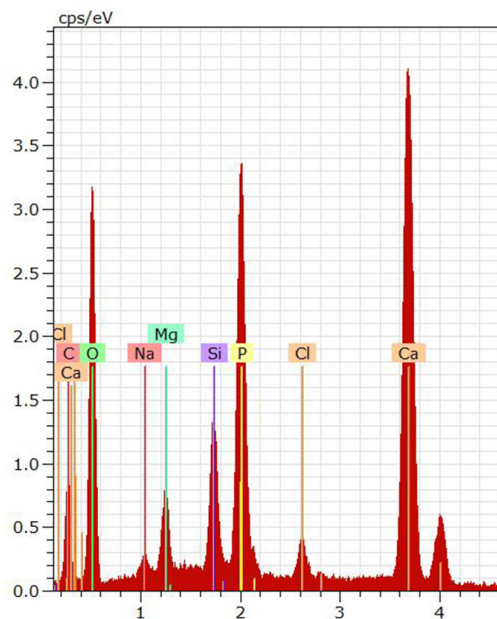


Fig. 5. EDS data for the ceramic surface, after soaking in SBF for 7 days.

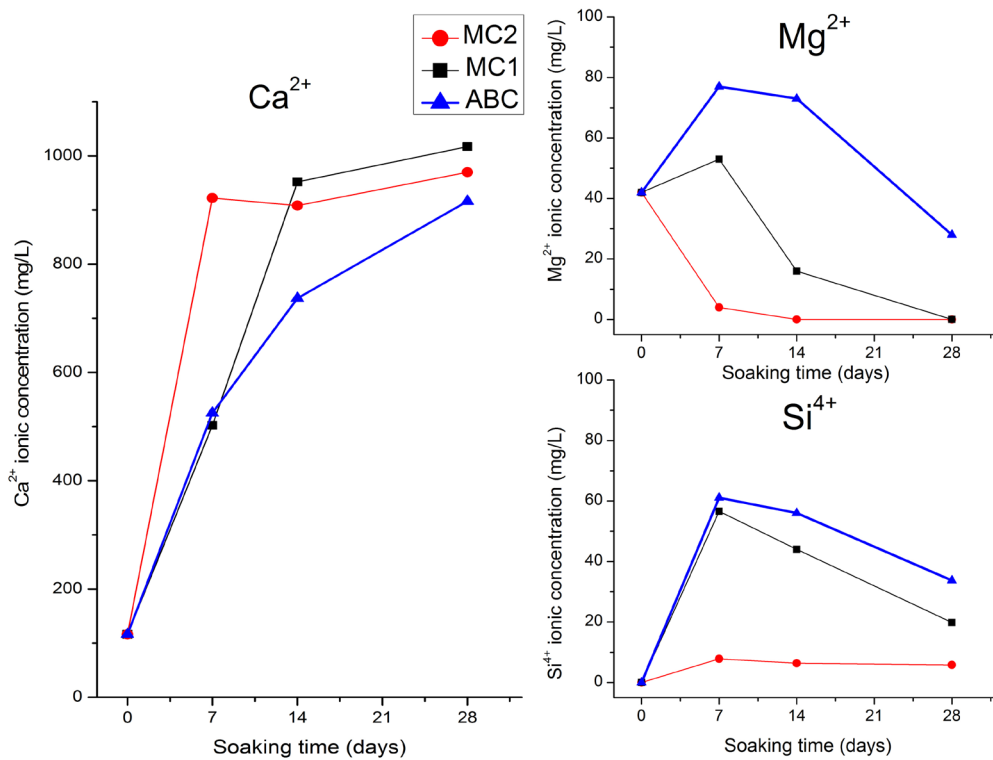


Fig. 6. Evolution of elemental concentrations of Ca, Mg and Si in SBF solution measured by ICP-OES for different soaking times of ceramics ÅBC, MC1 and MC2.

ceramics (MC1), regardless of the higher calcium content in merwinite compared to that in åkermanite. Therefore, ÅBC exhibits a higher solubility for the above test duration. The relative difference in the amount of magnesium release is the largest one, with a magnesium concentration 45% higher compared to the test of MC1. Magnesium ions are thought to inhibit the formation of HA [25, 26], but our experimental data gives almost similar results for the newly formed phosphate layer on the surface of both ceramics. The following ratios of calcium and phosphorus on the surface of both samples were recorded by the EDS: MC1 (Ca:P = 2.03), while that for ÅBC was calculated as (Ca:P = 2.11).

After soaking in SBF for 14 days, changes related to the evolution of the apatite layer formed on the surface of MC1 and ÅBC are observed. Various trends in ion concentrations in the SBF are registered. Calcium release from MC1 is higher compared to that from ÅBC, however the magnesium concentration in the solution in contact with MC1 is 4.5 times lower. Throughout the *in vitro* test, there is an increase of the calcium concentration in the SBF solution. With the increase of time of soaking from 7 up to 28 days there is a decrease in the concentrations of magnesium and silicon, albeit at a different pace.

The sample designated as MC2 is a polyphase ceramics with a chemical composition corresponding to merwinite and MC1, respectively, but obtained at a lower temperature: 1100 °C. MC2 contains larnite, merwinite, åkermanite and periclase. The experimental data for all the three ceramic samples reveal their good capacity to form hydroxyapatite (HA), but apart from some differences in the morphology of the formed layer, Fig. 6 shows differences in the separation of ions in the SBF solution, which presume differences in the behavior of these ceramics in biological environment.

CONCLUSIONS

The preparation and the *in vitro* bioactivity of polyphase åkermanite-based ceramics were studied. The formation of a bone-like apatite layer on the surface after soaking in a simulated body fluid (SBF) for 7 days was proved.

The apatite forming ability of synthesized ceramics is high and close to that described in the literature on pure phase åkermanite ceramics, and also comparable to that of merwinite ceramics. The obtained results confirm that in the CaO-MgO-SiO₂ system a wide range of materials, differing in

chemical and phase composition, exhibit high *in vitro* bioactivity. Therefore, the opportunity should be explored to obtain bioceramic materials with varying phase content and structure, but the same chemical composition, in view of their optimization (improvement) for different applications.

REFERENCES

1. C. Wu, J. Chang, *J. Biomed. Mater. Res. Part B*, **83B**, 153 (2007).
2. X. Chen, J. Ou, Y. Wei, Z. Huang, Y. Kang, G. Yin, *J. Mater. Sci. Mater. Med.*, **21**, 1463 (2010).
3. M. Diba, O.-M. Goudouri, F. Tapia, A. R. Boccaccini, *Curr. Opin. Solid State Mater. Sci.*, **18**, 147 (2014).
4. K. Marzban, S. M. Rabiee, *Nanomed. Res. J.*, **2**, 1 (2017).
5. T. Nonami, S. Tsutsumi, *J. Mater. Sci., Mater. Med.*, **10**, 475 (1999).
6. N. Y. Iwata, G. H. Lee, Y. Tokuoka, N. Kawashima, *Colloids Surf. B*, **34**, 239 (2004).
7. Y. Huang, X. G. Jin, X. L. Zhang, H. L. Sun, J. W. Tu, T. T. Tang, et al. *Biomaterials*, **30**, 5041 (2009).
8. F. Shamoradi, R. Emadi, H. Ghomi, *J. Alloys Compd.*, **693**, 601 (2017).
9. A. K. Sharafabadi, M. Abdollahi, A. Kazemi, A. Khandan, N. Ozada, *Mater. Sci. Eng., C*, **71**, 1072 (2017).
10. X. Chen, G. Yin, J. Ou, H. Zhu, *J. Funct. Mater.*, **38**, 435 (2007).
11. M. Hafezi, A. Reza Talebi, S. Mohsen Miresmaeili, F. Sadeghian, F. Fesahat, *Ceram. Int.*, **39**, 4575 (2013).
12. C. T. Wu, J. Chang, W. Y. Zhai, S. Y. Ni, *J. Mater. Sci. Mater. Med.*, **18**, 857 (2007).
13. Y. Zhou, C. Wu, X. Zhang, P. Han, Y. Xiao, *J. Mater. Chem. B*, **1**, 3380 (2013).
14. W. Zhai, H. Lu, C. Wu, L. Chen, X. Lin, K. Naoki, et al., *Acta Biomater.*, **9**, 8004 (2013).
15. J. Gillot, M. Roskosz, H. Leroux, F. Capet, P. Roussel, *J. Non-Cryst. Solids*, **357**, 3467 (2011).
16. I. K. Mihailova, L. Radev, V. A. Aleksandrova, I. V. Colova, I. M. M. Salvado, M. H. V. Fernandes, *Bulg. Chem. Commun.*, **47** 253 (2015).
17. I. Mihailova, L. Radev, V. Aleksandrova, I. Colova, I. M. M. Salvado, M. H. V. Fernandes, *J. Chem. Techn. Metall.*, **50** 502 (2015).
18. W. Kraus, G. Nolze, Powdercell2.4, Federal Institute for materials Research and Testing Rudower Chaussee 512485 Berlin, Germany.
19. T. Kokubo, H. Kushitani, S. Sakka, T. Kitsugi and T. Yamamuro, *J. Biomed. Mater. Res.*, **24**, 721 (1990).
20. R. Choudhary, S. Koppala, S. Swamiappan, *J. Asian Ceram. Soc.*, **3**, 173 (2015).
21. L. Kriskova, Y. Pontikes, O. Cizer, A. Malfliet, J. Dijkmans, B. Sels, K. Van Balen, B. Blanpain, *J. Am. Ceram. Soc.*, **97**, 3973 (2014).
22. M. S. Rutstein, W. B. White, *Am. Mineral.*, **56**, 877 (1971).
23. I. Rehman, W. Bonfield, *J. Mater. Sci.: Mater. Med.*, **8**, 1 (1997).
24. M. Cerruti, C. Morterra, *Langmuir*, **20**, 6382 (2004).
25. J. Ma, C. Z. Chen, D. G. Wang, J. H. Hu., *Mater. Lett.*, **65**, 130 (2011).
26. J. Ma, C. Z. Chen, D. G. Wang, X. Shao, C. Z. Wang, H. M. Zhang, *Ceram. Int.*, **38**, 6677 (2012).